MODIFICATIONS INDUCED IN PHOTOCURING OF BIS-GMA/TEGDMA BY THE ADDITION OF GRAPHENE NANOPLATELETS FOR 3D PRINTABLE ELECTRICALLY CONDUCTIVE NANOCOMPOSITES

R. Moriche[1,2]*, J. Artigas[1], L. Reigosa[1], M. Sánchez[1], S. G. Prolongo[1], A. Ureña[1]

[1]Materials Science and Engineering Area, University Rey Juan Carlos, Madrid, Spain.

[2]Departamento de Ingeniería y Ciencia de los Materiales y del Transporte,

Universidad de Sevilla, 41092 Sevilla, Spain.

*E-mail: rmoriche@us.es

Abstract

The incorporation of nanoreinforcement in photocurable polymeric matrices can strongly affect the degree of curing and properties of the final nanocomposites as well as the process parameters for 3D printing. Particularly, the addition of GNPs in contents from 1 up to 10 wt% limits the degree of curing to 60% in Bis-GMA/TEGDMA. The increase up to 10 wt% causes a diminution of ~20% in the mentioned property. Additionally, the maximum thickness that can be cured by UV light abruptly decreases with the GNPs content, being ~400 μm when using 1 wt% and below 20 μm for nanocomposites filled with 10 wt%. Above the percolation threshold, the electrical conductivity of the photocured monolayers is dependent on the curing time, making possible the use of this materials as self-sensor of the degree of curing in additive manufacturing technologies.

Keywords: A. nano composites, A. Polymer-matrix composites (PMCs), B. Curing, B. Electrical properties, graphene nanoplatelets.

1. Introduction

In recent years, additive manufacturing (AM) or 3D printing in polymers has attracted the increasing interest due to the flexibility, the reduction of waste and accuracy of the process [1]. Particularly, stereolithography (SLA) makes possible the construction of solidified parts by polymerizing UV curable resins layer by layer [2,3]. In this process, the thickness of the monolayers cured in each scan and the degree of curing [4] is crucial as delamination [5] or other defects can be caused in printed 3D parts. For this reason, the thickness of the cured sequential layers is an important parameter [6], as it is going to determine resolution and quality of the printed part, as sequential thinner layers will result in higher resolution; and it is also crucial to avoid mentioned delamination, as there is a minimum thickness to prevent it [5]. Frequently, modifications of the resins with the incorporation of different micro and nanoparticles is needed to achieve enhancement of properties or multifunfunctionality [7,8]. These micro or nanoparticles can strongly influence the UV curing process of the polymers, changing the maximum cured thickness per scan and the degree of curing because they can act as light scattering and shielding centers [6,9,10].

Carbon based nanoparticles, such as carbon nanotubes (CNTs) and graphene nanoplatelets (GNPs) have been widely used to achieve electrically and thermally conductive nanocomposites [11,12] to be used as thermal interface materials (TIMs) [13,14], conductive devices [15] and sensors for structural health monitoring (SHM) [16,17] applications.

In this work, the influence in the maximum curable thickness per scan, the degree of curing and electrical conductivity of GNPs reinforced photocurable nanocomposites are analyzed. The dependence on the nanoplatelets content and aspect ratios was also

studied in order to elucidate how these features conditioned the 3D printing and to stablish limits in technology.

2. Materials and methods

2.1. Materials

The polymeric matrix used in the present work was a mixture of Bisphenol A bis(2hydroxyl-3-methacryloxypropyl)ether (Bis-GMA) and triethyleneglycol dimethacrylate (TEGDMA) in a weight ratio 50:50. TEGDMA was used to reduce the high viscosity of Bis-GMA. The photopolimerization agent was camphorquinone (CQ) in a weight content of 0.7 %. In order to accelerate the polymerization of the resin, a concentration of 0.32 wt% of dimethylaminoethylmethacrylate (DMAEM) was added. All the chemicals listed above were purchased from *Eschem*.

Graphene nanoplatelets (GNPs) with different aspect ratios were used in order to analyze the effect on the UV curing process. Type *Grade 4* from *Cheap Tubes,* named in this work as LD5, has an average lateral size of ~ 5 μm and a thickness below 4 nm, with a specific surface area of 750 m^2/g. In contrast, type *M25* from *XGScience*, named in this paper as LD25, has an average lateral size of ~ 25 μm, an average thickness □ 6 nm, and a specific surface area of 120-150 m^2/g. It is important to note that none of the GNPs has been functionalized or has received any surface treatment.

2.2. Nanocomposites manufacturing

Nanoplatelets were dispersed in the mixture of Bis-GMA and TEGDMA by probe sonication (*UP400S, Hielscher*) for 30 minutes with a cycle of 0.5 s and 50 % of amplitude. With the aim of studying the inhibition of curing due to the incorporation of the GNPs into the polymer matrix, and based on previously published research [18,19], GNPs contents of 1, 3, 5 and 10 wt% were used. Once dispersion was completed, the photocuring agent and catalyst were added and, then, the mixture was again sonicated to ensure homogeneity for 1 minute.

After the procedure finished, the material was deposited on a glass substrate and UV-cured into a UV chamber (*Otoflash G171*). Curing time was set to 1, 2, 4 and 8 minutes and after that time, the non-cured portion was removed.

2.3. Characterization of UV-cured coatings

The thicknesses of the UV-cured layers were measured by optical profilometry in *a Zeta 20* model from *KLA-Tencor*. Scanning electron microscopy (SEM), a *Hitachi S4800 SEM-FEG*, was used to evaluate the dispersion degree of the GNPs into the epoxy matrix. Fourier transform infrared spectroscopy was used to evaluate the degree of conversion of the polymeric matrix. Degree of conversion (DC) was calculated from the intensity ratios of the peaks corresponding to C=C at 1636 cm^{-1} ($I_{C=C}$) and phenyl ring at 1608 cm^{-1} (I_{phr}) after the curing process (*f*) related to the uncured matrix (*0*) using the following equation [20]:

$$DC = 1 - \frac{\left(A_{C=C}/A_{ph}\right)_f}{\left(A_{C=C}/A_{ph}\right)_0}$$

Electrical resistance of the coatings was measured in a source-meter unit *KEITHLEY 2410*. Two copper electrodes were fixed on the surface using a line of silver paint to minimize the electrical contact resistance and were placed at a distance of 20 mm.

3. Results and discussion

3.1. Effect of GNPs content, curing time and aspect ratio on UV curable thickness

As it has been mentioned, stereolithography (SLA) is an additive manufacturing process that use photocurable polymers to build the part [21]. The addition of nanoreinforcement can strongly affect the curing of the Bis-GMA/TEGDMA mixture. To elucidate the limitations of photocurable nanocomposites in 3D printing, Figure 1 shows the maximum curable thickness as a function of the lateral dimensions of the GNPs and curing time.

When GNPs contents below 1 wt% are incorporated into the matrix, the cured thickness of the layers are in both cases higher than 150 □m with a curing time of 1 minute, this thickness can be increased with increasing the UV exposure time, reaching values in the order of 400 – 500 μm. Therefore, by using only 1 wt% of GNPs as filler, the maximum curable thickness diminishes more than 50% related to the neat polymer, which is more than 1 mm. The reason of this significant diminution is that, although a good dispersion of the GNPs is achieved (Figure 2), the GNPs act as centers of UV absorption and light dispersion [22,23] and therefore, as UV shielding [24,25]. In the case of using higher

GNPs contents as nanoreinforcement, the maximum thickness considerably diminishes, being less than 100 μm for 3 wt% and down to 10 μm when using more than 5 wt%. Additionally, an increment in the UV exposure time does not significantly increases the maximum thickness. This fact is slightly more pronounced in the case of using smaller lateral dimensions because the effective number of GNPs incorporated into the polymer is higher for a same weight percentage and it becomes more important when the content increases.

This effect strongly conditions the production rates of the parts as a major number of layers is needed to build the total thickness.

3.2. Conversion degree of nanoreinforced coatings

Another issue to take into account is the influence of the GNPs addition in the conversion degree of the Bis-GMA/TEGDMA polymer. As GNPs have been demonstrated to absorb and disperse the UV light, it can affect the conversion degree of the layers, causing a detriment of mechanical properties [26]. As an example, the use of montmorillonite nanoparticles as nanofiller in BisGMA/TEGDMA causes a diminution in DC from 72.6% down to 61.5%, when adding 20 vol% and 50 vol%, respectively [27].

Figure 3 shows representative FTIR spectra of all the samples as function of the curing time. It can be observed that the peak corresponding to C=C at 1636 cm^{-1} ($I_{C=C}$) diminishes with the curing time in all the cases because of a major degree of curing (DC)

[28]. This fact is negligible in nanocomposites reinforced with 5 wt% LD5 from 2 up to 8 minutes (Figure 3a), what means that an increment in time does not increase the DC. It is important also to point out that in nanocomposites reinforced with contents between

3-5 wt% of GNPs (Figure 3c-3f), as for LD5 and LD25, as well as for 1wt% LD25 (Figure 3b), an increase of the UV exposure time from 4 up to 8 minutes does not cause a significant decrease of the C=C peak, therefore, there is no meaningful change in DC.

In contrast, nanocomposites reinforced with 10 wt% (Figure 3g-3h), independently on the lateral dimensions of the GNPs, show an appreciable diminution of the mentioned intensity as a higher curing time is used, up to 8 minutes.

With the aim of comparing the calculated DC of the different nanocomposites, related to the uncured Bis-GMA/TEGDMA mixture, a process map is plotted in Figure 4. The maximum degree of curing achieved is ~ 60% in both types of GNPs and it is reached with GNPs contents below 5 wt% and curing times higher than 2 minutes. As it has been mentioned above, using contents higher than 3 wt% considerably reduces the maximum curable thickness of the system and, consequently, also the DC. Similar results have been reported by Sangermano et al. [7], who also attributed this effect to UV light shielding of GNPs.

Additionally, the use of low curing times causes the reduction of the DC in ~ 20%. This issue does not limit 3D printing but makes evident the necessity of post-curing to achieve high mechanical properties and thermal stability, if needed, once the part is printed by stereolithography.

One issue to consider is that the reinforcement with GNPs contents higher than 5 wt% provokes the DC to be less than 50%, including nanocomposites cured for 8 minutes. This is caused by the strong scattering and absorption of UV light by the presence of the GNPs. In contrast with the thickness, the addition of GNPs with higher lateral dimensions causes lower DC values for high UV exposure times. This can be due to the fact that higher lateral dimensions result in higher UV absorption, while GNPs with lower lateral dimensions provoke higher light reflection due to a higher quantity of 2D nanoplatelets [29],

achieving a higher DC [30]. This strong absorption of carbon based reinforcement has been previously reported by other authors such as González et at. [31], who observed a strong absorption of light by the addition of CNTs, which causes a lower conversion and rate of photopolymerization.

3.3. Electrical conductivity of nanoreinforced coatings

The main aim of analyzing changes induced in photocuring of the polymer nanocomposites by the addition of the GNPs is to achieve 3D printable conductive devices. For this reason, the electrical resistance of cured samples with a GNPs content above the percolation threshold for both, LD5 and LD25 GNPs, is discussed.

Figure 5 shows the I-V curve for layers reinforced with 10 wt%. A decrease in the electrical resistance caused by a major crosslinking of the polymeric matrix was detected. This may be caused because of an enhanced GNP/matrix interphase, which causes the reduction of the interparticle electrical resistance.

One important issue to be noticed is the lower electrical resistance achieved by the addition of LD25 nanoplatelets. This is due to the larger lateral dimensions of the GNPs [15], which makes easier the formation of the electrical network facilitating the electrical contact between overlying GNPs.

As the electrical resistance is dependent on the degree of curing, it can be used as monitoring system during the process to measure DC. Figure 6 shows the evolution of the electrical resistance of layers reinforced with a GNPs content of 10 wt% correlated to the DC as a function of the UV exposure time. When LD5 GNPs are used as nanofiller (Figure 6a), the layers are not electrically conductive until the UV exposure time reaches 4 minutes, this fact means that there is a threshold in curing time, i.e. DC. In the case of

LD25 nanoplatelets (Figure 6b), the electrically conductive films are achieved for 1 minute of curing time, although the DC is lower. This can be explained by the difference in the lateral dimensions, which makes easier, as explained above the formation of the electrical network.

As mentioned before, once the system becomes electrically conductive, the electrical resistance diminishes with a higher crosslinking of the polymeric matrix and, thus, the DC can be monitored. Although a deep study is needed to correlate changes in electrical resistance to DC, it has been demonstrated its potential application as monitoring system for curing in 3D printing technologies, as stereolithography.

As conclusion, Figure 7 shows all the studied properties for the nanocomposites reinforced with a GNPs content of 10 wt%. It can be seen that the use of GNPs with lower lateral dimensions leads to higher DC values, while the use of GNPs with higher lateral dimensions makes possible to achieve lower electrical resistances and higher photocured maximum thickness, what can increase the production rate of 3D printed parts.

4. Conclusions

The influence of the addition of GNPs in the curing process of photocurable polymers for 3D printing has been analyzed. It has been demonstrated that the maximum thickness of the monolayer formed by the GNP-based photocurable nanocomposites is strongly conditioned by the GNPs content and the UV exposure time. The influence of UV exposure time becomes more significant for low GNPs contents. In contrast, the influence of UV curing time in DC is more substantial in high GNPs contents, stabilizing at lower times for low GNPs contents. Although both, thickness and DC are also dependent on the lateral size of GNPs, this parameter has more influence in the electrical conductivity of

the nancomposites and DC than in the maximum thickness. The use of GNPs with lower lateral size permits to obtain higher DC but lower electrical conductivities than the use of GNPs with higher lateral size. Additionally, it was found that the electrical conductivity of the photocured layers is dependent of the DC, making possible the use of the nanocomposites as self-monitoring system for 3D printing technologies.

5. Acknowledgement

The authors would like to thank the *Ministerio de Economía y Competitividad* of *Spain Government* (Project MAT2016-78825-C2-1-R) and *Comunidad de Madrid Government* (P2013/MIT-2862).

6. References

[1] X. Wang, M. Jiang, Z. Zhou, J. Gou, D. Hui, 3D printing of polymer matrix composites: A review and prospective, Compos. Part B Eng. 110 (2017) 442–458. doi:10.1016/j.compositesb.2016.11.034.

[2] W. Gao, Y. Zhang, D. Ramanujan, K. Ramani, Y. Chen, C.B. Williams, C.C.L. Wang, Y.C. Shin, S. Zhang, P.D. Zavattieri, The status, challenges, and future of additive manufacturing in engineering, Comput. Des. 69 (2015) 65–89. doi:10.1016/j.cad.2015.04.001.

[3] M. Vatani, Y. Lu, E.D. Engeberg, J.W. Choi, Combined 3D printing technologies and material for fabrication of tactile sensors, Int. J. Precis. Eng. Manuf. 16

(2015) 1375–1383. doi:10.1007/s12541-015-0181-3.

[4] T.A. Akopova, P.S. Timashev, T.S. Demina, K.N. Bardakova, N. V. Minaev, V.F. Burdukovskii, G. V. Cherkaev, L. V. Vladimirov, A. V. Istomin, E.A. Svidchenko, N.M. Surin, V.N. Bagratashvili, Solid-state synthesis of unsaturated chitosan derivatives to design 3D structures through two-photon-induced polymerization, Mendeleev Commun. 25 (2015) 280–282. doi:10.1016/j.mencom.2015.07.017.

[5] X. Tian, W. Zhang, D. Li, J.G. Heinrich, Reaction-bonded SiC derived from resin precursors by Stereolithography, Ceram. Int. 38 (2012) 589–597. doi:10.1016/j.ceramint.2011.07.047.

[6] Z. Weng, Y. Zhou, W. Lin, T. Senthil, L. Wu, Structure-property relationship of nano enhanced stereolithography resin for desktop SLA 3D printer, Compos. Part A Appl. Sci. Manuf. 88 (2016) 234–242. doi:10.1016/j.compositesa.2016.05.035.

[7] M. Sangermano, L. Calvara, E. Chiavazzo, L. Ventola, P. Asinari, V. Mittal, R. Rizzoli, L. Ortolani, V. Morandi, Enhancement of electrical and thermal conductivity of Su-8 photocrosslinked coatings containing graphene, Prog. Org. Coatings. 86 (2015) 143–146. doi:10.1016/j.porgcoat.2015.04.023.

[8] C. Esposito Corcione, R. Striani, F. Montagna, D. Cannoletta, Organically modified montmorillonite polymer nanocomposites for stereolithography building process, Polym. Adv. Technol. 26 (2015) 92–98. doi:10.1002/pat.3425.

[9] C. Sciancalepore, F. Moroni, M. Messori, F. Bondioli, Acrylate-based silver nanocomposite by simultaneous polymerization–reduction approach via 3D stereolithography, Compos. Commun. 6 (2017) 11–16. doi:10.1016/j.coco.2017.07.006.

[10] Y. Han, F.K. Wang, H. Wang, X. Jiao, D. Chen, High-strength boehmite-acrylate composites for 3D printing: Reinforced filler-matrix interactions, Compos. Sci. Technol. 154 (2018) 104–109. doi:10.1016/j.compscitech.2017.10.026.

[11] C. Ramirez, L. Garzón, P. Miranzo, M.I. Osendi, C. Ocal, Electrical conductivity maps in graphene nanoplatelet/silicon nitride composites using conducting scanning force microscopy, Carbon N. Y. 49 (2011) 3873–3880. doi:10.1016/j.carbon.2011.05.025.

[12] S. Chandrasekaran, C. Seidel, K. Schulte, Preparation and characterization of graphite nano-platelet (GNP)/epoxy nano-composite: Mechanical, electrical and thermal properties, Eur. Polym. J. 49 (2013) 3878–3888. doi:10.1016/j.eurpolymj.2013.10.008.

[13] H. Rong, W.-Q.Q. Lin, J.-C.C. Zheng, M. Lu, Thermal characterization of a bridge-link carbon nanotubes array used as a thermal adhesive, Int. J. Adhes. Adhes. 49 (2014) 58–63. doi:10.1016/j.ijadhadh.2013.12.006.

[14] A.J. McNamara, Y. Joshi, Z.M. Zhang, Characterization of nanostructured thermal interface materials – A review, Int. J. Therm. Sci. 62 (2012) 2–11. doi:10.1016/j.ijthermalsci.2011.10.014.

[15] M.S. Kim, Y.B. Song, J.I. Park, Y.B. Park, J. Song, Prediction of twodimensional electrical conductivity of graphene/polymer composites, in: 18th Int. Conf. Compos. Mater., 2011: pp. 1–4.

[16] S. Luo, W. Obitayo, T. Liu, SWCNT-thin-film-enabled fiber sensors for lifelong structural health monitoring of polymeric composites - From manufacturing to utilization to failure, Carbon N. Y. 76 (2014) 321–329. doi:10.1016/j.carbon.2014.04.083.

[17] R. Moriche, M. Sánchez, A. Jiménez-Suárez, s. G. Prolongo, A. Ureña,

Electrically conductive functionalized-GNP / epoxy based composites : From nanocomposite to multiscale glass fibre composite material, Compos. Part B Eng. 98 (2016) 49–55. doi:10.1016/j.compositesb.2016.04.081.

[18] S.G. Prolongo, R. Moriche, a. Jiménez-Suárez, M. Sánchez, a. Ureña, Advantages and disadvantages of the addition of graphene nanoplatelets to epoxy resins, Eur. Polym. J. 61 (2014) 206–214. doi:10.1016/j.eurpolymj.2014.09.022.

[19] M. Sánchez, R. Moriche, X.F. Sánchez-Romate, S.G. Prolongo, J. Rams, A. Ureña, Effect of graphene nanoplatelets thickness on strain sensitivity of nanocomposites: A deeper theoretical to experimental analysis, Compos. Sci. Technol. 181 (2019) 107697. doi:10.1016/j.compscitech.2019.107697.

[20] J. He, E. Söderling, L.V.J. Lassila, P.K. Vallittu, Incorporation of an antibacterial and radiopaque monomer in to dental resin system, Dent. Mater. 28 (2012) e110–e117. doi:10.1016/j.dental.2012.04.026.

[21] L.F. Velásquez-garcía, S. Member, SLA 3-D Printed Arrays of Miniaturized , Internally Fed , Polymer Electrospray Emitters, 24 (2015) 2117–2127.

[22] A.Y. Vul, E.D. Eydelman, L. V. Sharonova, A.E. Aleksenskiy, S. V. Konyakhin, Absorption and scattering of light in nanodiamond hydrosols, Diam. Relat. Mater. 20 (2011) 279–284. doi:10.1016/j.diamond.2011.01.004.

[23] L. Rodrigues de Menezes, E. Oliveira da Silva, The Use of Montmorillonite Clays as Reinforcing Fillers for Dental Adhesives, Mater. Res. 19 (2016) 236–242.

[24] X. Tang, M. Tian, L. Qu, S. Zhu, X. Guo, G. Han, K. Sun, X. Hu, Y. Wang, X. Xu, Functionalization of cotton fabric with graphene oxide nanosheet and polyaniline for conductive and UV blocking properties, Synth. Met. 202 (2015) 82–88. doi:10.1016/j.synthmet.2015.01.017.

[25] X. Hu, M. Tian, L. Qu, S. Zhu, G. Han, Multifunctional cotton fabrics with graphene/polyurethane coatings with far-infrared emission, electrical conductivity, and ultraviolet-blocking properties, Carbon N. Y. 95 (2015) 625–633. doi:10.1016/j.carbon.2015.08.099.

[26] M.N. dos Santos, C. V. Opelt, F.H. Lafratta, C.M. Lepienski, S.H. Pezzin, L.A.F. Coelho, Thermal and mechanical properties of a nanocomposite of a photocurable epoxy-acrylate resin and multiwalled carbon nanotubes, Mater. Sci. Eng. A. 528 (2011) 4318–4324. doi:10.1016/j.msea.2011.02.036.

[27] L.M.P. Campos, L.C. Boaro, T.M.R. Santos, P.A. Marques, S.R.Y. Almeida, R.R. Braga, D.F. Parra, Evaluation of flexural modulus, flexural strength and degree of conversion in BISGMA/TEGDMA resin filled with montmorillonite nanoparticles, J. Compos. Mater. 51 (2017) 927–937. doi:10.1177/0021998316656925.

[28] W. Cao, Y. Zhang, X. Wang, Y. Chen, Q. Li, X. Xing, Y. Xiao, X. Peng, Z. Ye, Development of a novel resin-based dental material with dual biocidal modes and sustained release of Ag+ions based on photocurable core-shell AgBr/cationic polymer nanocomposites, J. Mater. Sci. Mater. Med. 28 (2017). doi:10.1007/s10856-017-5918-3.

[29] L. Qu, M. Tian, X. Hu, Y. Wang, S. Zhu, X. Guo, G. Han, X. Zhang, K. Sun, X. Tang, Functionalization of cotton fabric at low graphene nanoplate content for ultrastrong ultraviolet blocking, Carbon N. Y. 80 (2014) 565–574. doi:10.1016/j.carbon.2014.08.097.

[30] B. Farkas, M. Rodio, I. Romano, A. Diaspro, R. Intartaglia, Fabrication of hybrid nanocomposite scaffolds by incorporating ligand-free hydroxyapatite

nanoparticles into biodegradable polymer scaffolds and release studies, Beilstein J. Nanotechnol. 6 (2015) 2217–2223. doi:10.3762/bjnano.6.227.

[31] G. Gonzalez, A. Chiappone, I. Roppolo, E. Fantino, V. Bertana, F. Perrucci, L. Scaltrito, F. Pirri, M. Sangermano, Development of 3D printable formulations containing CNT with enhanced electrical properties, Polymer (Guildf). 109 (2017) 246–253. doi:10.1016/j.polymer.2016.12.051.

Figure captions

Figure 1. Maximum photocurable thickness of GNP-based nanocomposites: (a) LD5 and (b) LD25.

Figure 2. SEM micrographs of the fracture surface of GNP-based nanocomposites (GNPs content of 5 wt%): (a) LD5 and (b) LD25.

Figure 3. FTIR spectra of GNP-based nanocomposites depending of the UV exposure time reinforced with (a, b) 1, (c, d) 3, (e, f) 5 and (g, h) 10 wt%: (a, c, e, g) LD5 and (b, d, f, h) LD25.

Figure 4. Degree of conversion of GNP-based coatings as function of the curing time and GNP content of GNP-based nanocomposites: (a) LD5 and (b) LD25.

Figure 5. Influence of curing time in the I-V characteristic curve of nanocomposite layers reinforced with 10 wt% of GNPs: (a) LD5 and (b) LD25.

Figure 6. Monitoring of UV curing of nanocomposite layers reinforced with 10 wt% of GNPs: (a) LD5 and (b) LD25.

Figure 7. Properties of nanocomposite layers reinforced with 10 wt% of GNPs: (a) LD5 and (b) LD25.

Figures

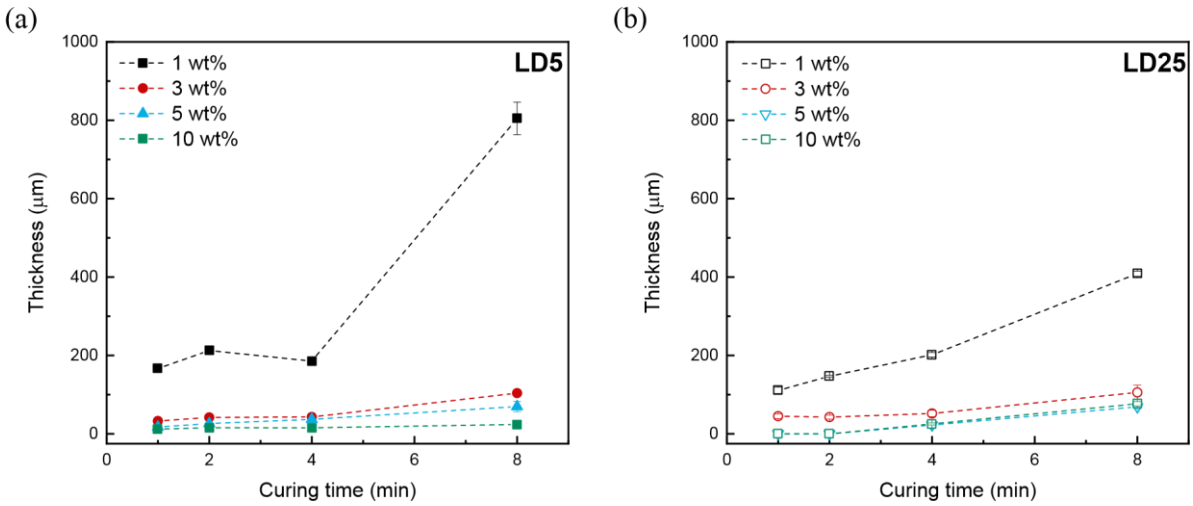

Figure 1. Maximum photocurable thickness of GNP-based nanocomposites: (a) LD5 and (b) LD25.

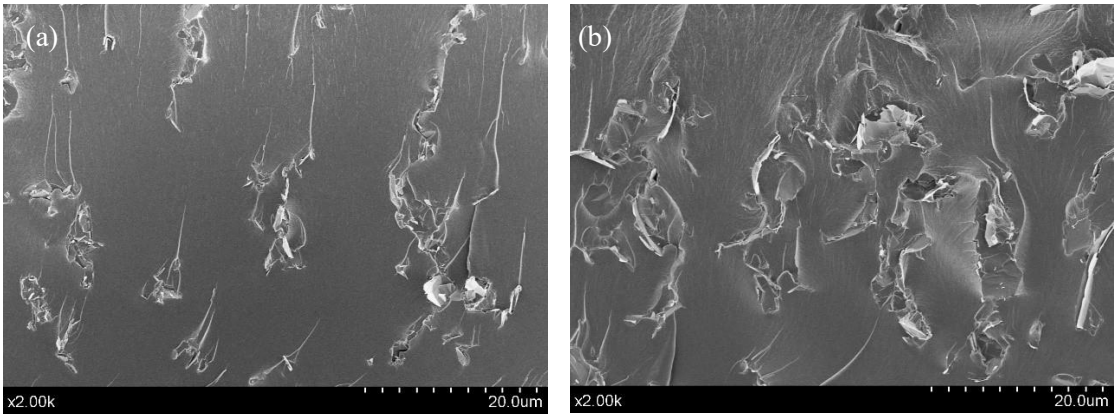

Figure 2. SEM micrographs of the fracture surface of GNP-based nanocomposites (GNPs content of 5 wt%): (a) LD5 and (b) LD25.

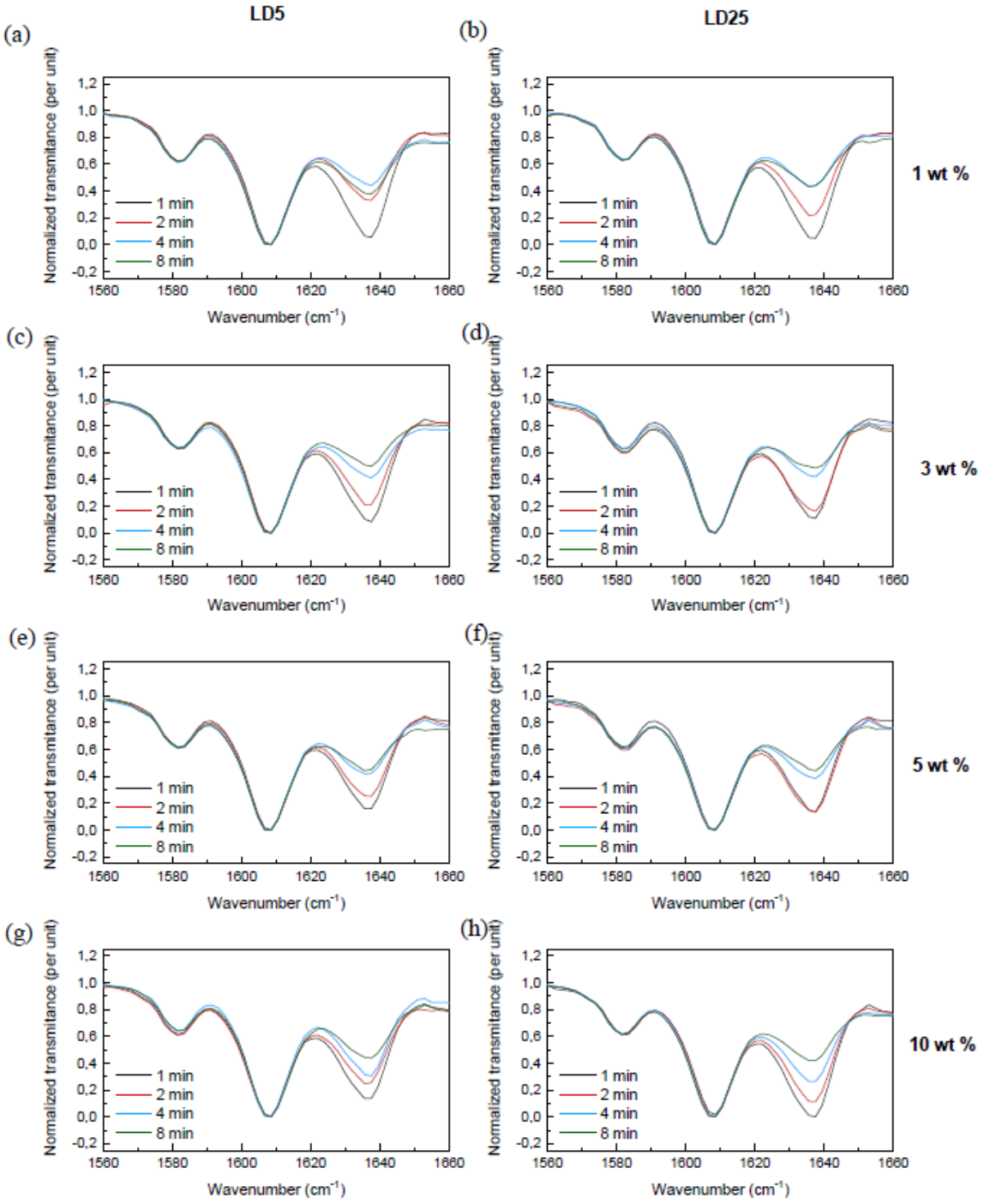

Figure 3. FTIR spectra of GNP-based nanocomposites depending of the UV exposure time reinforced with (a, b) 1, (c, d) 3, (e, f) 5 and (g, h) 10 wt%: (a, c, e, g) LD5 and (b, d, f, h) LD25.

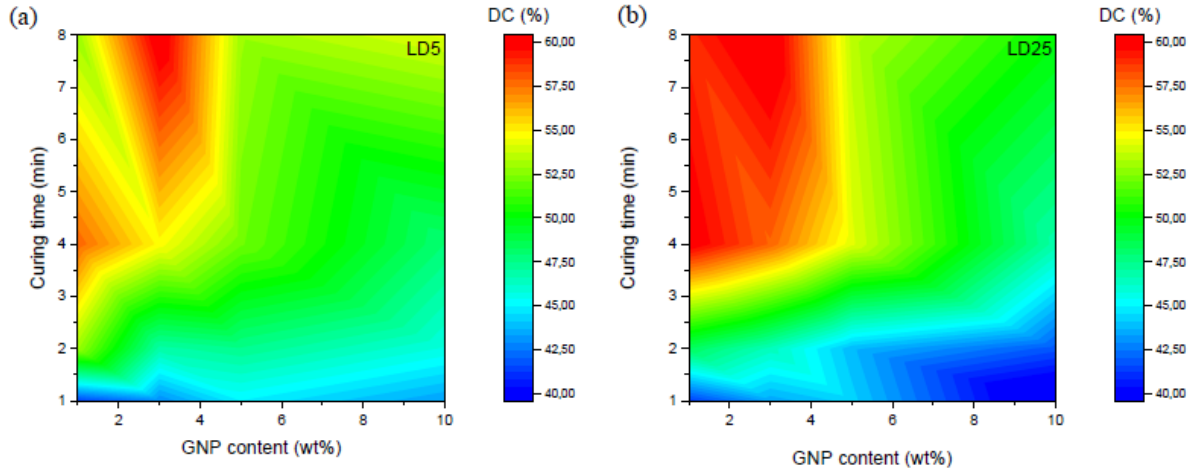

Figure 4. Degree of conversion of GNP-based coatings as function of the curing time and GNP content of GNP-based nanocomposites: (a) LD5 and (b) LD25.

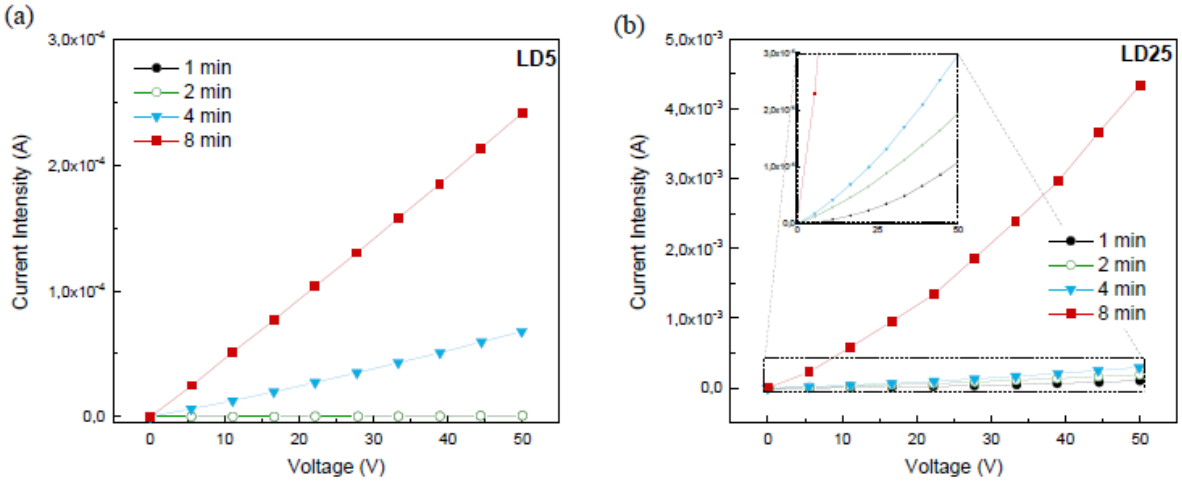

Figure 5. Influence of curing time in the I-V characteristic curve of nanocomposite layers reinforced with 10 wt% of GNPs: (a) LD5 and (b) LD25.

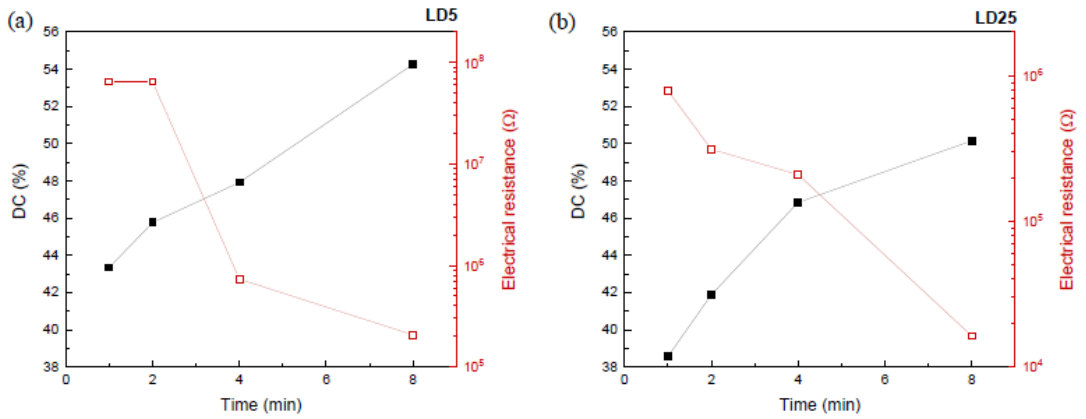

Figure 6. Monitoring of UV curing of nanocomposite layers reinforced with 10 wt% of GNPs: (a) LD5 and (b) LD25.

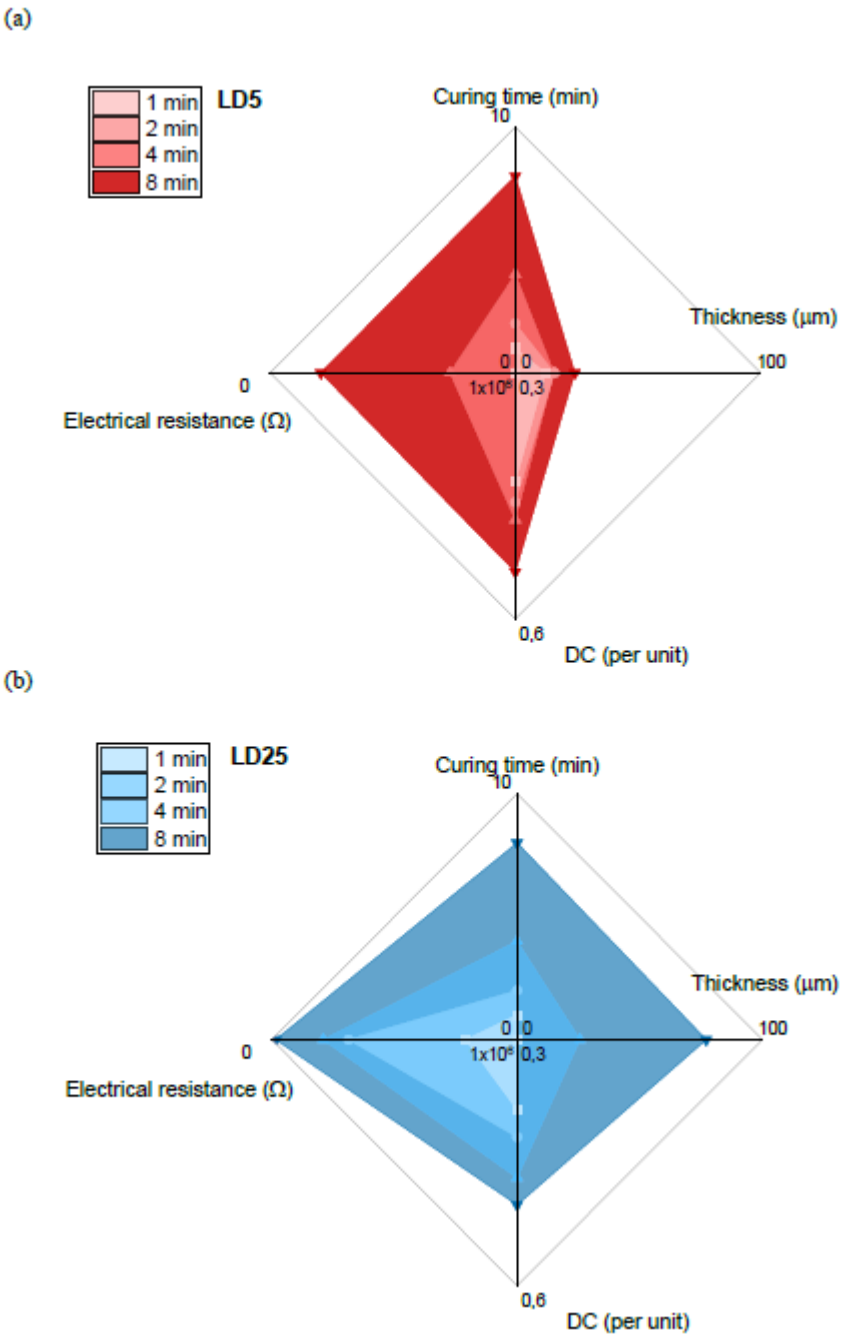

Figure 7. Properties of nanocomposite layers reinforced with 10 wt% of GNPs: (a) LD5 and (b) LD25.